RESEARCH ARTICLE

In Vivo Assessment of Neuroinflammation in 4-Repeat Tauopathies

Carla Palleis, MD,[1] Julia Sauerbeck,[2] Leonie Beyer, MD,[2] Stefanie Harris,[2] Julia Schmitt,[2]
Estrella Morenas-Rodriguez, PhD,[3] Anika Finze,[2] Alexander Nitschmann,[2] Francois Ruch-Rubinstein,[2]
Florian Eckenweber,[2] Gloria Biechele,[2] Tanja Blume, MSc,[3] Yuan Shi, PhD,[3] Endy Weidinger, MD,[1] Catharina Prix, MD,[1]
Kai Bötzel, MD,[1] Adrian Danek, MD,[1] Boris-Stephan Rauchmann, MD,[4,8] Sophia Stöcklein, MD,[4]
Simon Lindner, PhD,[2] Marcus Unterrainer, MD,[4] Nathalie L. Albert, MD,[2] Christian Wetzel, PhD,[5] Rainer Rupprecht, MD,[5]
Axel Rominger, MD,[2,6] Peter Bartenstein, MD,[2,7] Jochen Herms, MD,[3,8] Robert Perneczky, MD,[3,9,10]
Christian Haass, PhD,[3,6,11] Johannes Levin, MD,[1,3,11]* Günter U. Höglinger, MD,[3,11,12]* and Matthias Brendel, MD[2,11]*

[1]Department of Neurology, University Hospital of Munich, Ludwig-Maximilians-Universität (LMU) Munich, Munich, Germany
[2]Department of Nuclear Medicine, University Hospital of Munich, LMU Munich, Munich, Germany
[3]German Center for Neurodegenerative Diseases, Munich, Germany
[4]Department of Radiology, University Hospital of Munich, LMU Munich, Munich, Germany
[5]Department of Psychiatry and Psychotherapy, University of Regensburg, Regensburg, Germany
[6]Department of Nuclear Medicine, University of Bern, Inselspital, Bern, Switzerland
[7]Chair of Metabolic Biochemistry, Biomedical Center, Faculty of Medicine, LMU Munich, Munich, Germany
[8]Center for Neuropathology and Prion Research, University Hospital of Munich, LMU Munich, Munich, Germany
[9]Department of Psychiatry and Psychotherapy, University Hospital, LMU Munich, Munich, Germany
[10]Ageing Epidemiology Research Unit, School of Public Health, Imperial College, London, UK
[11]Munich Cluster for Systems Neurology (SyNergy), Munich, Germany
[12]Department of Neurology, Hannover Medical School, Hannover, Germany

ABSTRACT: Background: Neuroinflammation has received growing interest as a therapeutic target in neurodegenerative disorders, including 4-repeat tauopathies. **Objectives:** The aim of this cross-sectional study was to investigate 18 kDa translocator protein positron emission tomography (PET) as a biomarker for microglial activation in the 4-repeat tauopathies corticobasal degeneration and progressive supranuclear palsy.

Methods: Specific binding of the 18 kDa translocator protein tracer ^{18}F-GE-180 was determined by serial PET during pharmacological depletion of microglia in a 4-repeat tau mouse model. The 18 kDa translocator protein PET was performed in 30 patients with corticobasal syndrome (68 ± 9 years, 16 women) and 14 patients with progressive supranuclear palsy (69 ± 9 years, 8 women), and 13 control subjects (70 ± 7 years, 7 women). Group

***Correspondence to:** Dr. Johannes Levin, Department of Neurology University of Munich & German Center for Neurodegenerative Diseases e.V., Marchioninstraße 15, 81377 Munich, Germany, E-mail: johannes.levin@med.uni-muenchen.de; or Dr. Günter Höglinger, Department of Neurology, Medizinische Hochschule Hannover, Carl-Neuberg-Str. 1, 30625 Hannover, Germany; E-mail: guenter.hoeglinger@dzne.de; or Dr. Matthias Brendel, MHBA, Department of Nuclear Medicine, University of Munich; Marchioninstraße 15, 81377 Munich, Germany, E-mail: matthias.brendel@med.uni-muenchen.de

Carla Palleis, Julia Sauerbeck contributed equally as first authors; Johannes Levin, Günter U. Höglinger, and Matthias Brendel contributed equally as last authors

comparisons and associations with parameters of disease progression were assessed by region-based and voxel-wise analyses.

Results: Tracer binding was significantly reduced after pharmacological depletion of microglia in 4-repeat tau mice. Elevated 18 kDa translocator protein labeling was observed in the subcortical brain areas of patients with corticobasal syndrome and progressive supranuclear palsy when compared with controls and was most pronounced in the globus pallidus internus, whereas only patients with corticobasal syndrome showed additionally elevated tracer binding in motor and supplemental motor areas. The 18 kDa translocator protein labeling was not correlated with parameters of disease progression in corticobasal syndrome and progressive supranuclear palsy but allowed sensitive detection in patients with 4-repeat tauopathies by a multiregion classifier.

Conclusions: Our data indicate that ^{18}F-GE-180 PET detects microglial activation in the brain of patients with 4-repeat tauopathy, fitting to predilection sites of the phenotype. The 18 kDa translocator protein PET has a potential for monitoring neuroinflammation in 4-repeat tauopathies. © 2020 The Authors. *Movement Disorders* published by Wiley Periodicals LLC on behalf of International Parkinson and Movement Disorder Society

Key Words: corticobasal syndrome; four-repeat tauopathies; progressive supranuclear palsy; sTREM2; translocator protein

Four-repeat (4R) tauopathies encompass a variety of neurodegenerative diseases,[1] including the movement disorders corticobasal syndrome (CBS)[2] and progressive supranuclear palsy (PSP).[3] Both are devastating neurodegenerative disorders, leading to death on average within 6 to 10 years after symptom onset.[1] The majority of patients with CBS and PSP referred to autopsy are characterized by intracellular aggregates of 4R tau in neurons and astroglia.[1]

Neuroinflammation plays a major role in 4R tauopathies, although there are ongoing debates on the cause and effect of glial contribution to disease.[4] Recovering reduced phagocytic activity of microglia late in the disease course reduces tau spreading in human brain tissue and mouse models,[5,6] but microglia and the inflammasome contribute to tau spreading by increasing its propagation and aggregation.[7,8] Thus, a better understanding of the role of neuroinflammation across different disease stages will be key for developing effective therapeutic strategies. Biomarkers allowing quantification of neuroinflammation in 4R tauopathies could ultimately unravel associations between neuroinflammation and clinical progression in vivo, resulting in a monitoring tool for immunomodulatory therapies.

Despite the incremental use of 18 kDa translocator protein positron emission tomography (TSPO-PET) imaging in Alzheimer's disease[9] and β-amyloid mouse models,[10,11] only 2 studies were performed so far in 4R tauopathies,[12,13] both reporting higher ^{11}C-PK11195 binding in the subcortical target regions of patients with PSP compared with controls. The detailed role of TSPO as a biomarker of activated microglia in relation to the different 4R tauopathy phenotypes and clinical progression has yet to be explored. Furthermore, ^{11}C labeled radiotracers likely hamper the translation of study results into clinical practice or therapeutic trials because of the short half-life. The triggering receptor on myeloid cells 2 (TREM2) is an important biomarker of neuroinflammation,[14] but despite upregulation in the substantia nigra of deceased patients with PSP,[15] there are no relevant reports on the relevance of TREM2 in 4R tauopathies yet.

Thus, we aimed to investigate the potential of ^{18}F-GE-180 TSPO-PET as a biomarker of microglial activation in 4R tauopathies. Pharmacological depletion of microglia was performed in a 4R tau mouse model to validate the specificity of the tracer. Dynamic scanning and noninvasive kinetic modeling in a subset of patients served to determine short acquisition windows for low patient burden and cost-effective TSPO-PET imaging. Finally, we recruited a substantial number of patients with 4R tauopathy and controls to test the capability of ^{18}F-GE-180 TSPO-PET to detect elevated microglia activation in patients with CBS and PSP and to study associations of TSPO labeling with parameters of disease progression. TREM2 and the albumin quotient were assessed in cerebrospinal fluid (CSF) to compare ^{18}F-GE-180 TSPO-PET quantification with markers of disease associated microglia and blood–brain barrier integrity.

Material and Methods

TSPO-PET Imaging Before and After Microglia Depletion in a 4R Tau Mouse Model

All animal experiments were performed in compliance with the National Guidelines for Animal Protection, Germany, and with the approval of the regional animal committee (Regierung von Oberbayern) overseen by a veterinarian. Small animal PET (μPET) experiments were carried out in 5 female human tau P301S mice, a mouse line expressing the human 0N4R tau isoform with the P301S mutation in exon 10 of *MAPT* gene under control of the murine thy1 promoter.[16] Strong elevation of TSPO labeling in the brainstem, the

cerebellum, the hippocampus, and the cortex of P301S mice versus wild-type at 6.5 months of age was observed previously.[17] TSPO-μPET examinations were performed at baseline (7 months of age) and during microglial depletion after PLX5622 administration for 7 weeks. The sample size calculation was based on the in-house TSPO-PET quantification in the same model[17] with the baseline acting as control to archive a power (1–β) of 0.80 at α of 0.05. PLX5622 was provided by Plexxikon (Berkeley, CA) and formulated in AIN-76A standard chow by Research Diets (New Brunswick, NJ) at 1200 ppm. μPET imaging was performed as reported previously.[18] After coregistration to a magnetic resonance imaging (MRI) mouse atlas as described previously,[19] normalization of images to standardized uptake value (SUV) images was conducted. Predefined bilateral cortical (24 mm^3), brainstem (12 mm^3), and whole brain (500 mm^3) target volumes of interest were used, and SUVs were compared between baseline and follow-up. Details are provided in the Supporting Information.

Study Design, Study Population, and Clinical Assessments

A total of 30 patients with possible (n = 12) or probable (n = 18) CBS, 14 patients with possible (n = 1) or probable (n = 13) PSP–Richardson syndrome according to Armstrong Clinical Research and Movement Disorders Society criteria, respectively,[2,20] and 13 β-amyloid negative control subjects without objectified cognitive impairment and with intact motor function were included in the analysis at the Ludwig-Maximilians-Universität (LMU) Munich between September 2017 and January 2020 (Fig. S1, Table 1). A total of 3 patients with 4R tauopathy (n = 2 CBS, n = 1 PSP) and 1 control were excluded prior to the analysis as a result of low-affinity TSPO binding as revealed by genotyping

of the rs6971 single nucleotide polymorphism (SNP). Exclusion of low-affinity binders was performed because of lower ^{18}F-GE-180 binding in controls when compared with controls with medium-affinity or high-affinity binding status (unpublished data). Only patients who were β-amyloid negative and controls were included in the analysis. A total of 9 patients with CBS were excluded as a result of β-amyloid positivity in ^{18}F-flutemetamol PET, and 4 patients with PSP because of a non-Richardson syndrome/non-CBS phenotype prior to the analysis. The study and the data analyses (ethics applications 17–569, 17–755, and 19–022) were approved by the local ethics committee (LMU-Munich, Germany). All participants provided written informed consent according to the Declaration of Helsinki. Clinical data were collected according to the German multicenter prospective ProPSP cohort study.[21] Disease duration was defined as the time between symptom onset and PET imaging. The PSP Rating Scale (PSPRS) served as the disease severity parameter, and the Montreal Cognitive Assessment (MoCA) was used to assess the severity of cognitive deficits. Schwab and England Activities of Daily Living were recorded as a global score of functional ability.

Human PET Imaging
TSPO-PET Acquisition and Preprocessing

Patients were scanned at the Department of Nuclear Medicine, LMU, using a Biograph 64 PET/CT scanner (Siemens, Erlangen, Germany) and a bolus injection of 189 ± 12 MBq ^{18}F-GE-180. Details are provided in the Supporting Information. ^{18}F-GE-180 PET imaging was performed in a full dynamic setting (0–90 minutes post injectionem) for a mixed population of 11 patients with 4R tauopathies (6 CBS, 5 PSP) to allow noninvasive kinetic modeling and evaluation of a suitable time window for patient comfort and economic imaging. All

TABLE 1. Demographics at the group level

Demographics	4RT	CBS	PSP-RS	Controls
n	44	30	14	13
Age	68.3 ± 8.6	68.3 ± 9.1	68.8 ± 8.0	70.3 ± 7.5
Sex	24 ♀ / 20 ♂	16 ♀ / 14 ♂	8 ♀ / 6 ♂	7 ♀ / 6 ♂
rs6971	HAB: 30 / MAB: 14	HAB: 22 / MAB: 8	HAB: 8 / MAB: 6	HAB: 5 / MAB: 8
PSPRS	31.8 ± 13.4	29.7 ± 13.4	36.5 ± 12.7	n.a.
Disease duration (m)	32.7 ± 26.0	30.8 ± 21.9	36.7 ± 33.8	n.a.
MoCA	22.4 ± 5.7	22.4 ± 4.7 [a]P = 0.001	22.2 ± 7.8 [a]P = 0.004	29.1 ± 1.0
SEADL	60.0 ± 18.2	60.7 ± 18.0	58.6 ± 19.2	n.a.
Armstrong criteria	–	12 possible CBS, 18 probable CBS	–	–
MDS PSP criteria	–	7 not fulfilled, 4 suspected PSP-CBS, 19 possible PSP-CBS	1 possible PSP, 13 probable PSP	–

[a]Significant group differences between CBS and PSP groups against controls followed by the specific P value.
Demographics were statistically tested by analysis of variance or χ^2 test.
Abbreviations: 4RT, 4-repeat tauopathies; CBS, corticobasal syndrome; PSP, progressive supranuclear palsy; RS, Richardson syndrome; HAB, high-affinity binder; MAB, medium-affinity binder; PSPRS, PSP Rating Scale; n.a., not available; m, months; n, sample size; MoCA, Montreal Cognitive Assessment; SEADL, Schwab and England Activities of Daily Living; MDS, Movement Disorder Society.
Data are presented as n or mean ± SD.

other patients and controls received a static 60-minute to 80-minute p.i. scan. The SUVs of the 60-minute to 80-minute p.i. images of all 44 patients with 4R tauopathies were averaged and compared with the average SUV of the 13 controls by calculating a percentage difference map. After visual and quantitative inspection (application of Hammers atlas regions), the bilateral antero-lateral temporal lobe was deemed suitable for further evaluation as a pseudo-reference tissue (distribution volume ratios: distribution volume ratio (DVR) and SUV ratios [SUVr]) as it showed no differences between patients with 4R tauopathies and controls and low variance. For dynamic data sets, the Logan reference tissue model in PMOD[22] was used to calculate DVR images (for details, see the Supporting Information).

TSPO-PET Data Analysis

The ^{18}F-GE-180 DVR and SUVr values were obtained in 7 subcortical target regions[23] defined by the atlas of the basal ganglia,[24] including an additional manually drawn midbrain target region[25] and 12 cortical target regions as predefined by the Hammer's atlas[26] in the Montreal Neurology Institute space. The selection of target regions was based on earlier autopsy studies.[27,28] All target regions are listed in Table 2. Single-frame SUVr values of dynamic data sets were correlated with 0-minute to 90-minute DVR deriving from Logan graphical analysis. For target region-based group analyses, the maximum ^{18}F-GE-180 SUVr value of bilateral target regions was used to account for potential side asymmetries.

Statistical parametric mapping (V8; University College of London, London, UK) running in Matlab version R2011a (MathWorks Inc., Natick, MA) was used for voxel-wise statistical analyses. Group comparisons of ^{18}F-GE-180 SUVr images of the full 4R tauopathy cohort as well as CBS and PSP patient groups versus controls were performed by an unpaired t test using age, sex, and the TSPO polymorphism as covariates. Topological false discovery rate correction for multiple comparisons[29] with a significance threshold of $P < 0.05$ was applied.

β-amyloid-PET Acquisition and Analysis

All CBS and control subjects underwent static ^{18}F-flutemetamol PET imaging from 90 to 110 minutes p.i. as described previously using the same PET scanner. Images were dichotomized into positive or negative by a visual read of a single nuclear medicine expert supported by regional z scores in the frontal, parietal, and temporal target regions as derived by the Gold software package (V4.17; HERMES Medical Solutions, Stockholm, Sweden).

DNA Extraction and SNP Genotyping

rs6971 SNP genotyping was performed as described previously (for details, see the Supporting Information).

sTREM2 and Albumin Measures

sTREM2 concentration was measured in the available CSF samples (18 patients with CBS and 12 controls) by a modified assay based on the previously described sTREM2 enzyme-linked immunosorbent assay using the MSD platform.[30,31] This assay was designed to selectively detect sTREM2 coming from cleavage of the full-length protein (for details, see the Supporting Information). Raw values are provided as ng/mL. The CSF/serum albumin ratio was measured as the gold-standard marker of blood–brain barrier integrity.

Statistics

SPSS (V25; IBM, Ehningen, Germany) was used for statistical testing. P values <0.05 were considered significant.

Mouse Study
^{18}F-GE-180 SUV of P301S mice were compared between baseline and microglial depletion by a paired Student t test.

Methodology
In the subset of human dynamic scans, the agreement between DVR and SUVr of different time frames was assessed by a Pearson coefficient of correlation (R). In the full human data set, coefficients of variance were calculated and compared between 60-minute and 80-minute p.i. ^{18}F-GE-180 SUV and SUVr (paired Student t test).

Demographics
Age, PSPRS, disease duration, and MoCA scores were compared between the different study groups (CBS, PSP, controls) by a 1-way analysis of variance, whereas sex and the rs6971 polymorphism were subject to a χ^2 test.

Group Comparisons
The ^{18}F-GE-180 SUVr of predefined target regions (maximum value of bilateral regions) were compared between the 4 study groups (4R tauopathies, CBS, PSP, controls) by a multivariate analysis of covariance including age, sex, and rs6971 polymorphism as covariates. False discovery rate correction for multiple brain regions as well as post hoc Bonferroni correction for multiple testing of groups was applied. For region-based classification, regional SUVr $\geq$ mean value +2 standard deviations of the controls were defined as positive. Here, 1 positive target region defined the subject as positive (dichotomous) and sensitivity and specificity of TSPO-PET for detection of CBS and PSP was calculated. A summed z score vector was calculated for all patients with 4R tauopathies by the addition of single-

TABLE 2. TSPO-PET quantification at the group level

Subcortical	4RT, n = 44	CBS, n = 30	PSP-RS, n = 14	HC, n = 13
Putamen	0.934 (0.904–0.963) [a]P = 0.009	0.940 (0.904–0.976) [a]P = 0.010	0.920 (0.868–0.973)	0.822 (0.767–0.876)
Globus pallidus externus	0.978 (0.949–1.007) [a]P = 0.001	0.987 (0.952–1.023) [a]P = 0.001	0.960 (0.908–1.011) [a]P = 0.038	0.831 (0.777–0.885)
Globus pallidus internus	1.047 (1.013–1.080) [a]P = 4.28e-5	1.048 (1.007–1.090) [a]P = 1.52e-4	1.043 (0.983–1.103) [a]P = 0.002	0.843 (0.781–0.906)
Thalamus	1.031 (0.999–1.062)	1.042 (1.003–1.081)	1.008 (0.951–1.064)	0.949 (0.890–1.008)
Subthalamic nucleus	1.112 (1.069–1.155) [a]P = 0.003	1.119 (1.066–1.172) [a]P = 0.004	1.097 (1.021–1.174) [a]P = 0.046	0.921 (0.842–1.001)
Substantia nigra	1.068 (1.035–1.101) [a]P = 0.004	1.068 (1.027–1.108) [a]P = 0.009	1.068 (1.009–1.127) [a]P = 0.042	0.926 (0.865–0.988)
Dentate nucleus	0.981 (0.946–1.015)	0.979 (0.935–1.022)	0.985 (0.922–1.047)	0.881 (0.817–0.946)
Midbrain	1.086 (1.049–1.122) [a]P = 0.005	1.087 (1.042–1.133) [a]P = 0.010	1.082 (1.016–1.148) [a]P = 0.049	0.936 (0.868–1.004)
Cortical	4RT, n = 44	CBS, n = 30	PSP-RS, n = 14	HC, n = 13
Precentral gyrus	0.917 (0.892–0.943)	0.928 (0.897–0.958) [a]P = 0.036	0.896 (0.852–0.941)	0.842 (0.796–0.889)
Superior frontal gyrus	0.881 (0.857–0.904)	0.892 (0.863–0.920)	0.858 (0.816–0.899)	0.827 (0.783–0.871)
Middle frontal gyrus	0.887 (0.863–0.912) [a]P = 0.020	0.894 (0.864–0.925) [a]P = 0.017	0.873 (0.829–0.917)	0.802 (0.756–0.847)
Inferior frontal gyrus	0.973 (0.951–0.995) [a]P = 0.028	0.974 (0.946–1.001) [a]P = 0.040	0.970 (0.931–1.010)	0.899 (0.858–0.940)
Straight gyrus	0.997 (0.964–1.029)	0.990 (0.949–1.030)	1.011 (0.952–1.069)	0.906 (0.846–0.967)
Anterior cingulate gyrus	0.959 (0.931–0.987)	0.965 (0.931–1.000)	0.946 (0.895–0.996)	0.905 (0.852–0.957)
Anterior orbital gyrus	1.104 (1.075–1.133)	1.096 (1.060–1.132)	1.119 (1.067–1.172)	1.036 (0.982–1.091)
Medial orbital gyrus	1.124 (1.096–1.151)	1.123 (1.089–1.157)	1.125 (1.076–1.174)	1.045 (0.994–1.095)
Lateral orbital gyrus	1.219 (1.176–1.263)	1.214 (1.160–1.268)	1.230 (1.152–1.308)	1.098 (1.017–1.179)
Posterior orbital gyrus	1.161 (1.131–1.190)	1.166 (1.129–1.202)	1.151 (1.097–1.204)	1.085 (1.030–1.140)
Postcentral gyrus	0.892 (0.868–0.916)	0.899 (0.870–0.929)	0.876 (0.833–0.920)	0.841 (0.796–0.886)
Parietal lobe	0.915 (0.892–0.937)	0.928 (0.901–0.955)	0.888 (0.848–0.927)	0.866 (0.824–0.907)

[a]Significant differences of patient groups against controls are followed by the specific P value.
Values represent regional group means of TSPO-PET standardized uptake value ratios (60-minute to 80-minute time window) and their 95% confidence intervals in predefined subcortical and cortical brain areas. P values were derived from multivariate analysis of variance with age, sex, and rs6971 polymorphism as covariates. All P values were false discovery rate corrected for multiple comparisons (n = 20 brain regions) and Bonferroni post hoc corrections for multiple study groups.
Abbreviations: TSPO-PET, translocator protein positron emission tomography; 4RT, 4-repeat tauopathies; CBS, corticobasal syndrome; PSP, progressive supranuclear palsy; RS, Richardson syndrome; HC, controls without objectified memory impairment and with intact motor function.

region z scores ([individual SUVr patient − mean value SUVr controls]/standard deviation SUVr controls). A total of 9 regions (putamen, external and internal parts of the globus pallidus, subthalamic nucleus, substantia nigra, midbrain, precentral gyrus, middle frontal gyrus, inferior frontal gyrus) with significant differences of TSPO-PET binding at the group level were included in the z score vector to obtain a global but 4R tauopathy–specific measure of microglial activation. A univariate analysis of covariance including age and sex as covariates was performed for comparison of log-transformed sTREM2 measures and the CSF/serum albumin ratio between patients with CBS and controls.

Correlation Analyses

Partial correlations were calculated for ^{18}F-GE-180 SUVr in predefined regions and the summed z score vector with clinical severity (PSPRS), disease duration, and MoCA controlled for age, sex, and rs6971 polymorphism, and including false discovery rate corrections for multiple tests in predefined regions (n = 60 tests) within CBS and PSP subgroups. Partial correlations were calculated for sTREM2 with clinical severity (PSPRS), disease duration, and MoCA controlled for age and sex. Flexible fitting models were calculated between the summed z score vector and sTREM2 or the CSF/serum albumin ratio for patients with CBS.

Results

Specificity of ^{18}F-GE-180 to 4R Tau–Associated Microglia and Implementation of an Efficient TSPO-PET Scan Protocol

P301S 4R tau mice were imaged before and after microglial depletion by a CSF1R inhibitor. CSF1R blocking strongly reduced ^{18}F-GE-180 binding in the whole brain of 5 P301S mice and model-specific target regions (Fig. 1A,B), indicating specific detection of activated microglia by the tracer. Immunohistochemistry confirmed microglial depletion >90% by Iba1.

Dynamic imaging in patients with 4R tauopathies indicated a moderate brain uptake and fast wash out in 4R tauopathy target regions and the temporal reference region (Fig. 1C). SUVr tended to plateau after 60 minutes postinjection (Fig. 1D), similar to earlier observations in rodents.[18] Agreement between Logan DVR from kinetic modeling and single-frame SUVr reached $R > 0.6$, starting >6 minutes postinjection and dropped toward $R < 0.5$ for frames >80 minutes postinjection (Fig. 1E). 60-minute to 80-minute SUVr overestimated 0-minute to 90-minute DVR by $22.2\% \pm 4.9\%$ (cortical) and $29.5\% \pm 11.0\%$ (subcortical), but both correlated in a near linear fashion for cortical ($R = 0.91$, $P < 0.001$) and subcortical ($R = 0.85$, $P < 0.001$) target regions (Fig. 1F). Visual
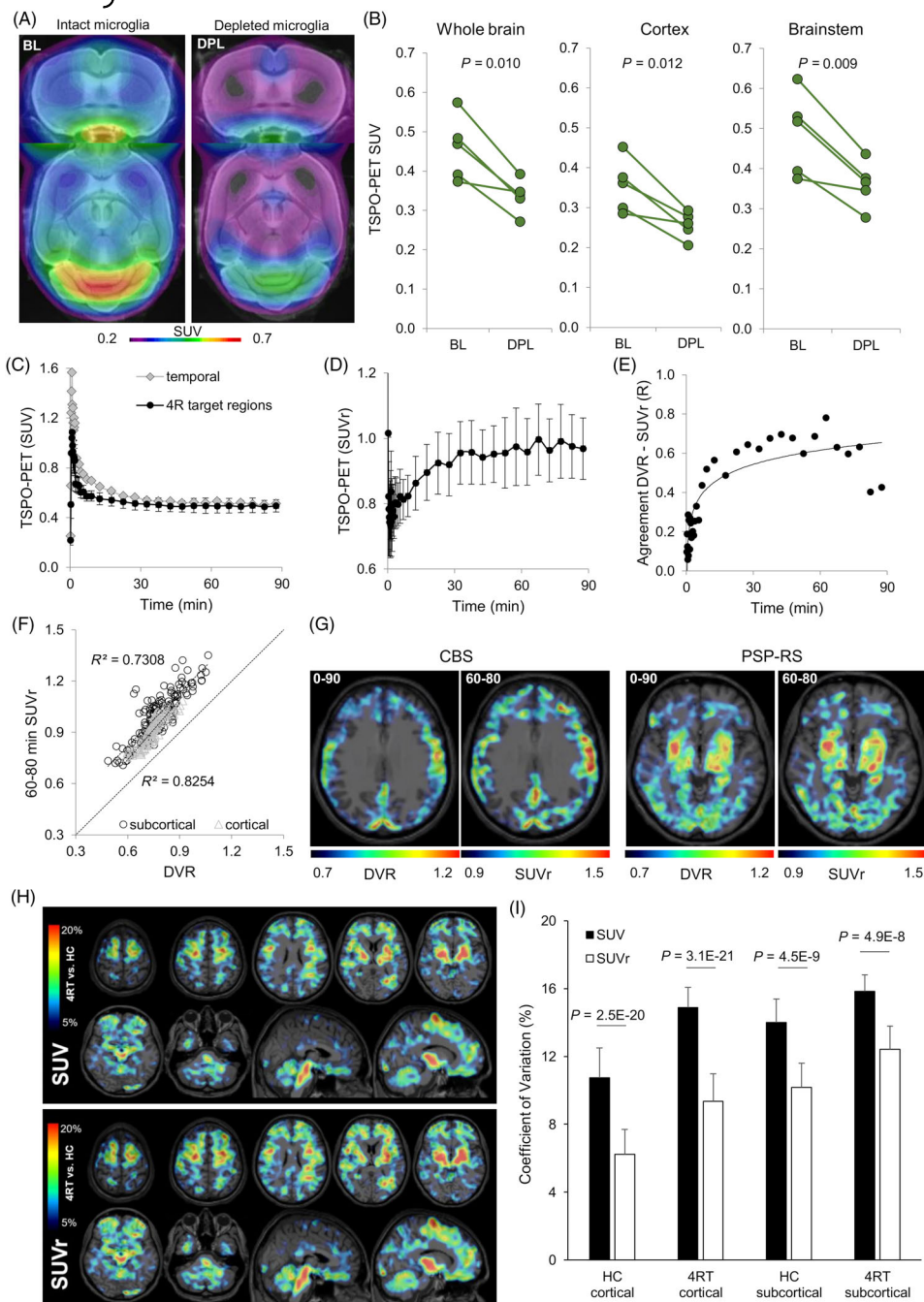
FIG. 1. Preclinical validation of tracer specificity and methodological considerations for human 4-repeat (4R) tauopathy translocator protein positron emission tomography (TSPO-PET) imaging. Mouse study: (**A**) Coronal (striatal layer) and axial ^{18}F-GE-180 TSPO-PET images of P301S mice on a magnetic resonance imaging standard template show strong decreases of the cerebral tracer uptake in week 7 of microglia depletion (DPL) when compared with baseline (BL). Images represent the average standardized uptake value (SUV) of n = 5 P301S mice. (**B**) Spaghetti plots show individual TSPO-PET SUV changes between baseline and a state of depleted microglia in target regions of P301S mice. P values are derived from paired Student t tests. Human study: Values derived from n = 11 4R tauopathy patients (n = 6 corticobasal syndrome, n = 5 progressive supranuclear palsy) (**C–F**). (**C**) Time-activity curves of 4R tauopathy target regions (mean value ± standard deviation of 19 brain regions) and a temporal lateral pseudo-reference tissue. (**D**) Time-activity ratio curves of 4R tauopathy target regions divided by binding in the pseudo-reference tissue (mean value ± standard deviation of 19 brain regions). (**E**) Agreement between distribution volume ratios (DVR) and SUV ratios (SUVr) in single frames during the 90-minute scan duration. Each dot represents the mean Pearson correlation coefficient (R) of 19 4R tauopathy target regions. (**F**) Agreement of DVR with 60-minute to 80-minute SUVr of cortical and subcortical 4R tauopathy target regions as quantified at the single patient level. (**G**) Individual examples of visual agreement between DVR and 60-minute to 80-minute SUVr for a patient with corticobasal syndrome (CBS; 58-year-old man; PSP Rating Scale, 27; disease duration, 37 months; Montreal Cognitive Assessment, 14) and a patient with progressive supranuclear palsy–Richardson syndrome (PSP-RS; 74-year-old man; PSP Rating Scale, 18; disease duration, 10 months; Montreal Cognitive Assessment, 22). Axial planes of ^{18}F-GE-180 TSPO-PET images are projected on a standard magnetic resonance imaging atlas. (**H**) Percentage difference maps of n = 44 4R tauopathy patients (4RT) and n = 13 healthy controls (HC) for SUV and SUVr quantification of the ^{18}F-GE-180 TSPO-PET group average. Percentage differences are projected in axial and sagittal planes on a standard magnetic resonance imaging atlas. (**I**) Coefficients of variance in the contrast of SUV and SUVr quantification. Bars represent mean Coefficients of variance values ± standard deviation of cortical (n = 12) and subcortical (n = 7) 4R tauopathy target regions. P values are derived from a paired Student t test. [Color figure can be viewed at wileyonlinelibrary.com]

image analysis revealed highly similar uptake patterns of DVR and SUVr maps for cortical and subcortical TSPO labeling in patients with 4R tauopathies (Fig. 1G). Percentage difference maps of SUV and SUVr indicated a high similarity of magnitude (Fig. 1H), but intersubject variance was significantly decreased in the control and 4R tauopathy groups by the SUVr approach (Fig. 1I).

TSPO Labeling Follows the Expected Topology in Patients with CBS and PSP

All demographics and disease parameter are provided in Table 1. There were no significant differences in age, sex, rs6971 polymorphism, disease severity, or disease duration between patients with CBS and PSP. Both 4R tauopathy patient groups were matched for age, sex, and rs6971 polymorphism when compared with controls. MoCA was significantly reduced in patients with CBS (22.4 ± 4.7, P = 0.001) and patients with PSP (22.2 ± 7.8, P = 0.004) when compared with controls (29.1 ± 1.0).

TSPO-PET SUVs in the temporal pseudo-reference region were not different between 4R tauopathy high-affinity binder (HAB; 0.52 ± 0.07), 4R tauopathy medium-affinity binder (MAB; 0.55 ± 0.09), control HAB (0.52 ± 0.07), and control MAB (0.54 ± 0.03; all P = nonsignificant; Fig. S2). Predefined regions of interest indicated significantly higher TSPO-PET SUVr in the subcortical (putamen, internal and external part of the globus pallidus, subthalamic nucleus, substantia nigra, and midbrain) and cortical brain areas (middle frontal gyrus and inferior frontal gyrus) of patients with 4R tauopathies when compared with controls after false discovery rate correction for multiple comparisons and adjustment for age, sex, and the rs6971 polymorphism (Table 2). The strongest elevation of TSPO-PET SUVr in the combined 4R tauopathy cohort was observed in the internal part of the globus pallidus (1.047; 95% confidence interval [CI], 1.013–1.080) when compared with controls (0.843; 95% CI, 0.781–0.906; P < 0.001, false discovery rate corrected; Table 2). Patients with CBS and PSP phenotypes indicated increased TSPO labeling in the majority of subcortical target areas when compared with controls (Table 2). The group of patients with a CBS phenotype also showed significantly elevated TSPO-PET SUVr versus controls in the cortical regions of the frontal lobe, including the precentral gyrus, the middle frontal gyrus, and the inferior frontal gyrus, whereas patients with a PSP phenotype did not show elevated cortical TSPO-PET SUVr versus control subjects (Table 2).

Statistical parametric mapping validated higher TSPO labeling in the entire group of patients with 4R tauopathies versus control subjects and were most pronounced in the midbrain and the pons, the globus pallidus, the dentate nucleus. Cortical areas of patients with 4R tauopathies indicated higher TSPO labeling when compared with controls and were most pronounced in the motor and supplemental motor cortices (Fig. 2A, Table S1A). Patients with CBS showed an elevated TSPO labeling in the cortical areas, including motor and supplemental motor cortices, whereas the patients with PSP did not. Subcortical TSPO labeling was increased in the CBS and PSP subgroups (compare Fig. 2B and Fig. 2C, Table S1B,C).

TSPO Labeling Allows Sensitive Detection of Patients with 4R Tauopathies and Occurs in Agreement with an Asymmetric CBS Phenotype

TSPO labeling in predefined regions of interest did not show associations with parameters of disease progression (Table S4, Supporting Information Results). A multiregion classifier indicated sensitivities of 80% and 79% for patients with CBS and PSP at a specificity of 92% (Fig. S3, Supporting Information Results).

Of 30 patients with CBS, 18 indicated a right peripheral predominance of clinical symptoms, 11 showed a predominant left phenotype, and 1 was affected equilaterally. Asymmetry indices of TSPO-PET in the subcortical regions showed a significant lateralization to the hemisphere contralateral of the clinical phenotype (49/77, χ^2 = 5.11, P = 0.024), with highest agreement in the internal (15/18, χ^2 = 8.10, P = 0.004) and external (9/9, χ^2 = 9.00, P = 0.003) parts of the globus pallidus. Asymmetry indices of TSPO-PET in the frontal cortex were not significantly associated with lateralization of the clinical phenotype (49/98, χ^2 = 1.98, P = 0.160).

sTREM2 Peaks at Low TSPO Labeling in CBS

A subpopulation of 18 patients with CBS and 12 controls was eligible for CSF sTREM2 measures. There was no difference in absolute sTREM2 levels between patients with CBS and controls (0.96 [95% CI, 0.89–1.04] vs. 0.96 [95% CI, 0.86–1.05], P = 0.950; Fig. 3A). Measures of sTREM2 in patients with CBS as a function of TSPO labeling described an inverted U-shape with a peak at low TSPO-PET signal in the combined and cortical target regions, but not in subcortical target regions (Fig. 3B,C, Supporting Information Fig. S4A). In TSPO-positive patients (>2 SD of controls), there was a negative linear association between TSPO labeling and sTREM2 (R = −0.616, P = 0.016). There was no significant association between parameters of disease progression and sTREM2 (Fig. 3D-F).

TSPO Labeling Is Not Associated with Blood–Brain Barrier Integrity

To test for a dependency of ^{18}F-GE-180 binding on dysfunctional blood–brain barrier integrity, we compared the CSF/serum albumin ratio with the individual z score vector of TSPO labeling in patients with CBS. There was no significant difference of the CSF/serum albumin ratio between patients with CBS and controls (6.8 [95% CI, 5.8–7.7] vs. 6.1 [95% CI, 4.6–7.6], $P = 0.501$; Fig. 3G). TSPO-PET z score vectors were not significantly different between 5 patients with CBS with dysfunctional blood–brain barriers and 20 patients with CBS with normal CSF/serum albumin ratios (16.0 [95% CI, 4.0–27.9] vs. 20.7 [95% CI, 15.2–26.2], $P = 0.480$; Fig. 3H). TSPO-PET z score vectors in patients with CBS and the CSF/serum albumin ratio did not show any significant associations (Fig. 3I,J, Fig. S4B).

Discussion

We provide the first human study using a fluorinated TSPO-PET radiotracer in a meaningful sized cohort of patients with CBS and PSP. Our translational data in a 4R tauopathy mouse model verified that ^{18}F-GE-180 detects 4R tau–related microglial activation with high specificity. Dynamic imaging and methodological workup in humans indicated feasibility of TSPO-PET imaging with low patient effort and simplified quantification approaches. Patients with CBS and PSP revealed elevated TSPO labeling in subcortical brain regions, whereas patients with CBS additionally showed stronger elevation of TSPO labeling in the forebrain. Cross-sectional correlation analyses indicated only minor associations of TSPO labeling with parameters of disease progression but a potential of TSPO-PET as an early disease stage biomarker in CBS.

To the best of our knowledge, there are only 2 published reports on TSPO-PET imaging in 4R tauopathies, both only including patients with PSP,[12,13] whereas our study is the first including CBS. A study from 2006 investigated a small cohort of 4 patients with PSP using ^{11}C-PK11195 and implementing serial imaging in 2 patients.[12] Their baseline findings of the strongest TSPO-PET increases in the basal ganglia and brainstem are in line with our observations in 14 patients with PSP, whereas we could not confirm differences in the frontal cortex. A more recent study scanned 16 patients with PSP with a mean PSPRS score of 40.8 with ^{11}C-PK11195 together with an equal number of patients with Alzheimer's disease and 13 controls and found higher TSPO labeling in the putamen, thalamus, and pallidum in the patients with PSP compared with controls, but no binding differences versus Alzheimer's disease.[13] Our regional findings in 14 patients with PSP of

similar disease severity (mean PSPRS score, 36.5) confirm the earlier observations using a third-generation TSPO tracer. Our novel TSPO-PET data in CBS mirror the subcortical findings of PSP, but reveal an additional elevation of TSPO labeling in the neocortex with the strongest signal in the motor and supplemental motor areas of the forebrain. This fits well to the pronounced cortical phenotype of CBS compared with PSP and is also in line with the concept of overlapping neuropathology among different 4R tauopathies.[32]

Recently, ^{18}F-GE-180 to assess TSPO labeling in patients with glioma and multiple sclerosis was criticized because of inferior image quality and limited uptake across the blood–brain barrier.[33-35] This reflects an important topic since blood–brain barrier integrity can be disturbed in neurodegenerative disorders.[36] Based on our preclinical experience, we were aware of a high correlation of the ^{18}F-GE-180 PET signal with immunohistochemistry in mouse models of neurodegenerative disorders despite the low brain penetration of the tracer.[11,18,37] Although we deemed it unlikely that a parallel blood–brain barrier phenomenon caused these strong associations, we made use of pharmacological microglial depletion to prove specificity of the tracer for activated microglia in presence of 4R tau. As expected, we observed a clear decrease of the ^{18}F-GE-180 PET signal in microglia depleted P301S mice when compared with their own individual baseline. This strongly supports the claim of a specific ^{18}F-GE-180 PET signal in vivo and recent human in vivo blocking data supported specific detection of microglia by this tracer further.[38] In addition, we did not find any association of the CSF/serum albumin ratio as the gold-standard marker for blood–brain barrier integrity and TSPO labeling. Thus, we have no evidence that a blood–brain barrier breakdown causes the binding patterns of ^{18}F-GE-180. Furthermore, the binding patterns fit to the neuropathological topologies of CBS and PSP in former autopsy studies.[27,39,40]

Including corrections for multiple comparisons, we did not find significant associations between measures of disease progression and regional TSPO labeling in CBS and PSP, controlling for age, sex, and rs6971 polymorphism. Yet, although our ^{18}F-GE-180 PSP findings did not reach significance, they were roughly in line with positive associations of ^{11}C-PK11195 binding and disease severity in a cohort of 16 patients with PSP, showing a similarly large interindividual heterogeneity of TSPO labeling at a given PSPRS score.[13] In contrast, the regional associations of TSPO labeling with parameters of disease progression in CBS showed an equal or higher TSPO-PET signal in the early stages of disease progression. This could indicate a saturation of microglial activation in the late stages of CBS, which is known in the presence of amyloidosis.[41] We found a sensitivity of 75% in patients with possible CBS and
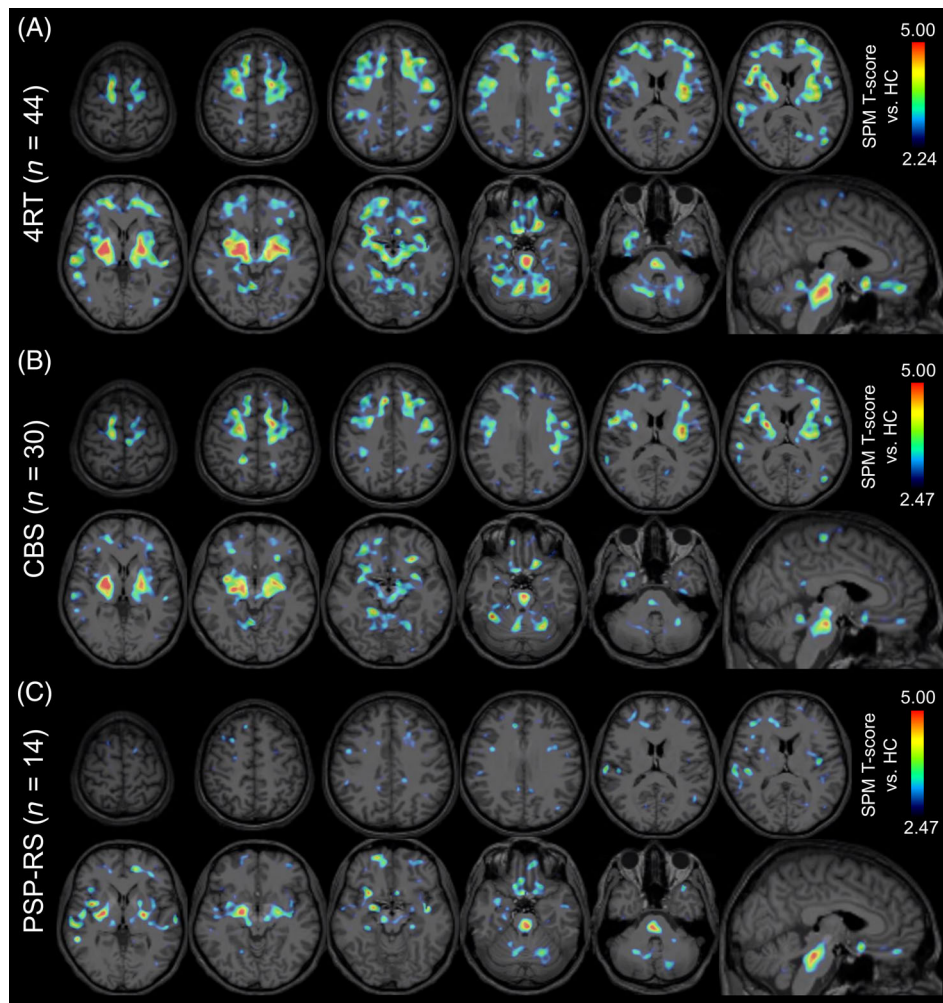
FIG. 2. Voxel-based differences of translocator protein positron emission tomography binding in 4R tauopathy patients. Color coding shows brain areas with increased translocator protein positron emission tomography binding in groups of all patients with (**A**) 4-repeat (4R) tauopathy (n = 44), (**B**) corticobasal syndrome (CBS; n = 30), and (**C**) progressive supranuclear palsy–Richardson syndrome patients (PSP-RS; n = 14) when compared with healthy controls (HC; n = 13). The *t* statistics are derived from an unpaired Student *t* test with age, sex, and rs6971 polymorphism as covariates as calculated by statistical parametric mapping (SPM). The lower threshold reflects a significance level of *P* = 0.05 after false discovery rate correction for multiple comparisons. The lower threshold for **C** was adjusted to **B** to improve visual comparability of differences in patients with CBS and PSP. Extracerebral voxels are masked. The T score maps are projected in axial and sagittal planes on a standard magnetic resonance imaging atlas. [Color figure can be viewed at wileyonlinelibrary.com]

even higher sensitivity for probable CBS and PSP versus controls using a simple semiquantitative multiregion classifier, underlining the potential of TSPO-PET as a supportive biomarker for diagnosis of 4R tauopathies and improving limited sensitivity of clinical diagnosis.[42] Despite the lacking association between TSPO labeling and parameters of disease progression, we find a clear agreement between asymmetries of subcortical TSPO labeling and contralateral clinical predominance of the CBS phenotype. This supports the important role of microglial activation in the pathophysiological cascade of 4R tauopathies.[4] A subpopulation of patients with CBS and controls was eligible for CSF sTREM2 measures, but missing differences between patients and controls suggest that CSF TREM2 measures appear less

sensitive when compared with a detailed work-up of TREM2 in brain regions in autopsy.[15] However, we find an interesting negative association between TSPO-PET and sTREM2 in patients with CBS after a sTREM2 peak at low levels of TSPO. Speculatively, this could indicate a functional burnout of microglia with increasing activity and deserves further longitudinal exploration. The observed cross-sectional heterogeneity of TSPO labeling in patients with 4R tauopathies will enable predictive analyses, aiming to elucidate if high or low TSPO labeling at baseline is associated with better clinical outcome. Taken together, longitudinal PET studies and predictive analyses of the clinical course are needed for further exploration of TSPO-PET as a biomarker in immunomodulatory trials. The current 4R
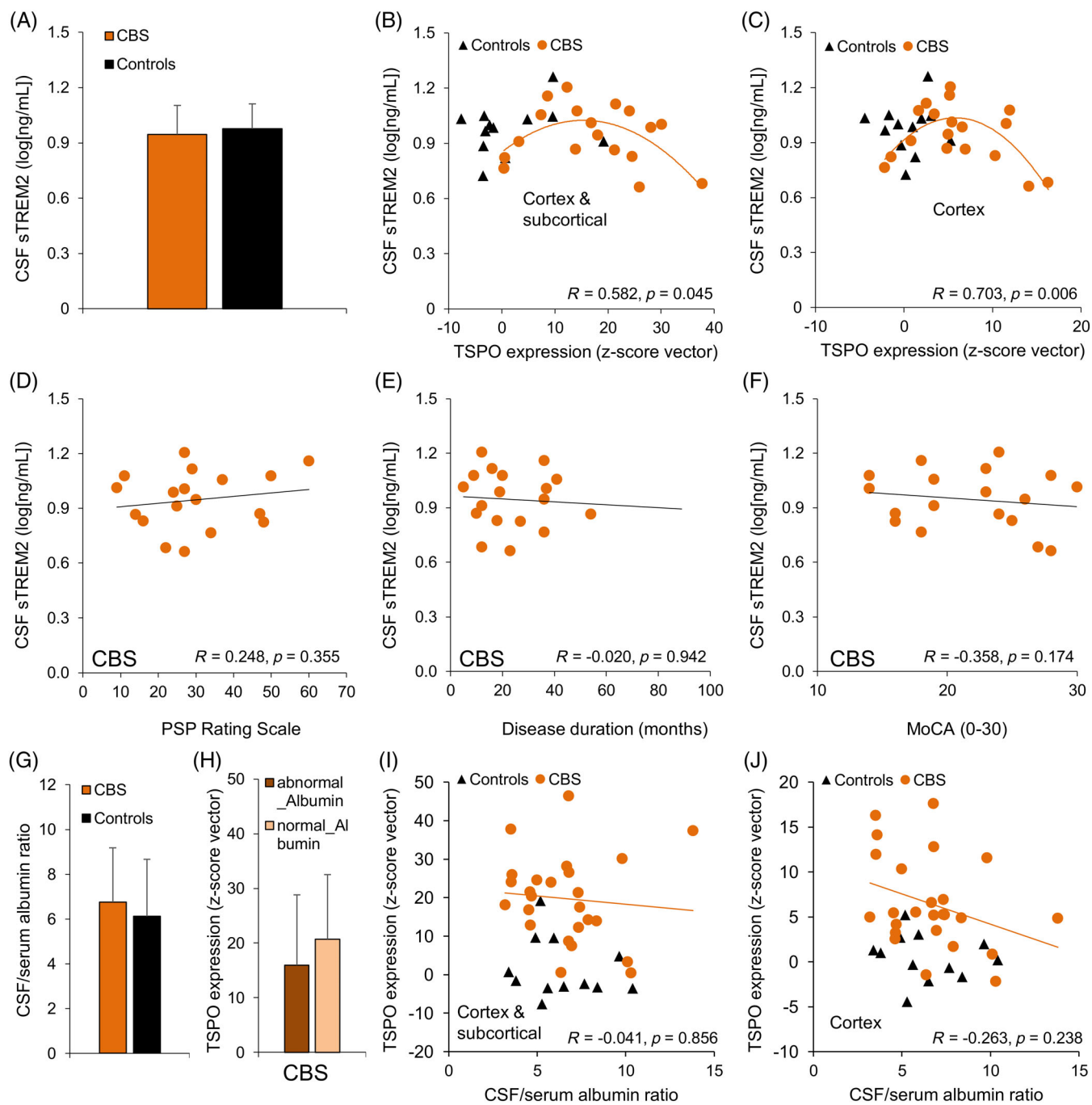
FIG. 3. Soluble triggering receptor on myeloid cells 2 (sTREM2) and blood–brain barrier integrity in patients with corticobasal syndrome (CBS). (**A**) Comparison of sTREM2 between patients with CBS and controls, controlled for age and sex. (**B,C**) Associations between multiregional translocator protein (TSPO) labeling and sTREM2 in patients with CBS for all brain regions with significant differences in TSPO– positron emission tomography (PET) (**B**) and a subanalysis in cortical regions (**C**). R/p values are derived from quadratic fits. (**D–F**) Associations between parameters of disease progression and sTREM2 in patients with CBS. (**G**) Comparison of the cerebrospinal fluid (CSF) to serum quotient of albumin (CSF/serum albumin ratio) between patients with CBS and controls. (**H**) Comparison of TSPO labeling between patients with CBS with an abnormal and a normal CSF/serum albumin ratio. Associations between the CSF/serum albumin ratio and multiregional TSPO labeling in patients with CBS for all brain regions with significant differences in TSPO-PET (l) and a subanalysis in cortical regions (**J**). R/p values are derived from partial correlation, controlled for age, sex, and rs6971. A subanalysis of subcortical regions is provided in Figure S4. MoCA, Montreal Cognitive Assessment. [Color figure can be viewed at wileyonlinelibrary.com]

tauopathy cohort will be followed clinically and by serial TSPO-PET to address this question.

Among the limitations of our study we note missing autopsy validation of the studied clinically diagnosed

4R tauopathy cases. However, the high specificity of a clinical 4R tauopathy diagnosis predicts a low number of false positive cases in the studied data set.[42] We acknowledge as another limitation that we did not

include arterial sampling in the dynamic imaging protocol, thus although we deem it unlikely, we cannot exclude effects from differences in plasma fractions and tracer metabolism among our study groups. Medium- and high-affinity binders were not equally distributed among the study groups. Since a subanalysis in medium- and high-affinity binders was not sufficiently powered, we included the binding status as a covariate, and we note that a remaining bias on the TSPO-PET quantification cannot be fully excluded. β-amyloid PET was not performed in the PSP arm of the study because of the high clinical probability of predicting a 4R tauopathy. Thus, we cannot rule out frequent[43] β-amyloid copathology and a subsequent impact on microglial activation in patients with PSP, which, however, does not have a major impact on clinical progression.

Conclusion

TSPO-PET imaging closely reflects the expected topology of microglial activation in 4R tauopathies and shows potential as a neuroinflammation biomarker. in vivo assessment of TSPO labeling has a potential to support early diagnosis of 4R tauopathies, facilitating increased sensitivity. Longitudinal studies are needed to explore the value of TSPO-PET imaging as a progression biomarker in 4R tauopathies. ●

References

1. Rosler TW, Tayaranian Marvian A, Brendel M, et al. Four-repeat tauopathies. Prog Neurobiol 2019;180:101644.

2. Armstrong MJ, Litvan I, Lang AE, et al. Criteria for the diagnosis of corticobasal degeneration. Neurology 2013;80(5):496–503.

3. Steele JC, Richardson JC, Olszewski J. Progressive supranuclear palsy. A heterogeneous degeneration involving the brain stem, basal ganglia and cerebellum with vertical gaze and pseudobulbar palsy, nuchal dystonia and dementia. Arch Neurol 1964;10:333–359.

4. Ferrer I, López-González I, Carmona M, et al. Glial and neuronal tau pathology in tauopathies: characterization of disease-specific phenotypes and tau pathology progression. J Neuropathol Exp Neurol 2014;73(1):81–97.

5. Martini-Stoica H, Cole AL, Swartzlander DB, et al. TFEB enhances astroglial uptake of extracellular tau species and reduces tau spreading. J Exp Med 2018;215(9):2355–2377.

6. Perea JR, Llorens-Martin M, Avila J, Bolos M. The role of microglia in the spread of tau: relevance for Tauopathies. Front Cell Neurosci 2018;12:172.

7. Asai H, Ikezu S, Tsunoda S, et al. Depletion of microglia and inhibition of exosome synthesis halt tau propagation. Nature neuroscience 2015;18(11):1584–1593.

8. Ising C, Venegas C, Zhang S, et al. NLRP3 inflammasome activation drives tau pathology. Nature 2019;575(7784):669–673.

9. Stefaniak J, O'Brien J. Imaging of neuroinflammation in dementia: a review. J Neurol Neurosurg Psychiatry 2016;87(1):21–28.

10. Liu B, Le KX, Park MA, et al. In vivo detection of age- and disease-related increases in neuroinflammation by 18F-GE180 TSPO MicroPET imaging in wild-type and Alzheimer's transgenic mice. J Neurosci 2015;35(47):15716–15730.

11. Parhizkar S, Arzberger T, Brendel M, et al. Loss of TREM2 function increases amyloid seeding but reduces plaque-associated ApoE. Nat Neurosci 2019;22(2):191–204.

12. Gerhard A, Trender-Gerhard I, Turkheimer F, Quinn NP, Bhatia KP, Brooks DJ. In vivo imaging of microglial activation with [11C](R)-PK11195 PET in progressive supranuclear palsy. Mov Disord 2006;21(1):89–93.

13. Passamonti L, Rodriguez PV, Hong YT, et al. [(11C)]PK11195 binding in Alzheimer disease and progressive supranuclear palsy. Neurology 2018;90(22):e1989–e1996.

14. Suarez-Calvet M, Kleinberger G, Araque Caballero MA, et al. sTREM2 cerebrospinal fluid levels are a potential biomarker for microglia activity in early-stage Alzheimer's disease and associate with neuronal injury markers. EMBO Mol Med 2016;8(5):466–476.

15. Sanchez-Ruiz de Gordoa J, Erro ME, Vicuna-Urriza J, et al. Microglia-related gene triggering receptor expressed in myeloid cells 2 (TREM2) is upregulated in the substantia nigra of progressive supranuclear palsy. Mov Disord 2020;35(5):885–890.

16. Allen B, Ingram E, Takao M, et al. Abundant tau filaments and non-apoptotic neurodegeneration in transgenic mice expressing human P301S tau protein. J Neurosci 2002;22(21):9340–9351.

17. Eckenweber F, Medina-Luque J, Blume T, et al. Longitudinal TSPO expression in tau transgenic P301S mice predicts increased tau accumulation and deteriorated spatial learning. J Neuroinflam 2020;17(1):208.

18. Brendel M, Probst F, Jaworska A, et al. Glial activation and glucose metabolism in a transgenic amyloid mouse model: a triple tracer PET study. J Nucl Med 2016;57:954–960.

19. Brendel M, Focke C, Blume T, et al. Time courses of cortical glucose metabolism and microglial activity across the life span of wild-type mice: a PET study. J Nucl Med 2017;58(12):1984–1990.

20. Hoglinger GU, Respondek G, Stamelou M, et al. Clinical diagnosis of progressive supranuclear palsy: the movement disorder society criteria. Mov Disord 2017;32(6):853–864.

21. Respondek G, Klockgether T, Spottke A, Höglinger G. German prospective studies on PSP: ProPSP and DESCRIBE-PSP. Poster presented at: Deutscher Kongress für Parkinson und Bewegungsstörungen, Düsseldorf; 2019. https://d-nb.info/1181570069/34. Accessed on November 15, 2020.

22. Logan J. A review of graphical methods for tracer studies and strategies to reduce bias. Nucl Med Biol 2003;30(8):833–844.

23. Brendel M, Barthel H, Van Eimeren T, et al. 18F-PI2620 tau-PET in progressive supranuclear palsy: a multi-center evaluation. JAMA Neurol 2020;77(11):1408–1419.

24. Keuken MC, Bazin PL, Backhouse K, et al. Effects of aging on T(1), T(2)*, and QSM MRI values in the subcortex. Brain Struct Funct 2017;222(6):2487–2505.

25. Brendel M, Schonecker S, Hoglinger G, et al. [(18)F]-THK5351 PET correlates with topology and symptom severity in progressive Supranuclear palsy. Front Aging Neurosci 2017;9:440.

26. Hammers A, Allom R, Koepp MJ, et al. Three-dimensional maximum probability atlas of the human brain, with particular reference to the temporal lobe. Hum Brain Mapp 2003;19(4):224–247.

27. Williams DR, Lees AJ. Progressive supranuclear palsy: clinicopathological concepts and diagnostic challenges. Lancet Neurol 2009;8(3):270–279.

28. Kovacs GG, Lukic MJ, Irwin DJ, et al. Distribution patterns of tau pathology in progressive supranuclear palsy. Acta Neuropathol 2020;140(2):99–119.

29. Chumbley J, Worsley K, Flandin G, Friston K. Topological FDR for neuroimaging. Neuroimage 2010;49(4):3057–3064.

30. Kleinberger G, Yamanishi Y, Suarez-Calvet M, et al. TREM2 mutations implicated in neurodegeneration impair cell surface transport and phagocytosis. Sci Transl Med 2014;6(243):243ra286.

31. Suarez-Calvet M, Morenas-Rodriguez E, Kleinberger G, et al. Early increase of CSF sTREM2 in Alzheimer's disease is associated with

tau related-neurodegeneration but not with amyloid-beta pathology. Mol Neurodegener 2019;14(1):1.

32. Höglinger GU. Is it useful to classify progressive supranuclear palsy and corticobasal degeneration as different disorders? Mov Disord Clin Pract 2018;5(2):141.

33. Zanotti-Fregonara P, Pascual B, Rostomily RC, et al. Anatomy of (18)F-GE180, a failed radioligand for the TSPO protein. Eur J Nucl Med Mol Imag 2020;47(10):2233–2236.

34. Zanotti-Fregonara P, Veronese M, Rizzo G, Pascual B, Masdeu JC, Turkheimer FE. Letter to the editor re: confirmation of specific binding of the 18-kDa translocator protein (TSPO) Radioligand [(18)F]GE-180: a blocking study using XBD173 in multiple sclerosis Normal appearing white and grey matter. Mol Imag Biol 2020;22(1):10–12.

35. Zanotti-Fregonara P, Veronese M, Pascual B, Rostomily RC, Turkheimer F, Masdeu JC. The validity of (18)F-GE180 as a TSPO imaging agent. Eur J Nucl Med Mol Imag 2019;46(6):1205–1207.

36. Farrall AJ, Wardlaw JM. Blood–brain barrier: ageing and microvascular disease–systematic review and meta-analysis. Neurobiol Aging 2009;30(3):337–352.

37. Kleinberger G, Brendel M, Mracsko E, et al. The FTD-like syndrome causing TREM2 T66M mutation impairs microglia function, brain perfusion, and glucose metabolism. EMBO J 2017;36(13):1837–1853.

38. Sridharan S, Raffel J, Nandoskar A, et al. Confirmation of specific binding of the 18-kDa translocator protein (TSPO) radioligand [18 F] GE-180: a blocking study using XBD173 in multiple sclerosis normal appearing white and grey matter. Mol Imag Biol 2019;21(5):935–944.

39. Williams DR, Holton JL, Strand C, et al. Pathological tau burden and distribution distinguishes progressive supranuclear palsy-parkinsonism from Richardson's syndrome. Brain 2007;130(Pt 6):1566–1576.

40. Dickson DW. Neuropathologic differentiation of progressive supranuclear palsy and corticobasal degeneration. J Neurol 1999;246(suppl 2):II6–1–II6–15.

41. Blume T, Focke C, Peters F, et al. Microglial response to increasing amyloid load saturates with aging: a longitudinal dual tracer in vivo muPET-study. J Neuroinflam 2018;15(1):307.

42. Respondek G, Grimm MJ, Piot I, et al. Validation of the movement disorder society criteria for the diagnosis of 4-repeat tauopathies. Mov Disord 2020;35(1):171–176.

43. Jecmenica Lukic M, Kurz C, Respondek G, et al. Copathology in progressive Supranuclear palsy: does it matter? Mov Disord 2020;35(6):984–993.

Supporting Data

Additional Supporting Information may be found in the online version of this article at the publisher's web-site.